F-Actin Aggregates in Transformed Cells

WILLIAM W. CARLEY, LARRY S. BARAK, and WATT W. WEBB
School of Applied Physics and Engineering, Cornell University, Ithaca, New York 14853

ABSTRACT Polymerized actin has been found aggregated into distinctive patches inside transformed cells in culture. The F-actin-specific fluorescent probe, nitrobenzoxadiazole-phallacidin, labels these F-actin aggregates near the ventral cell surface of cells transformed by RNA or DNA tumor viruses, or by chemical mutagens, or spontaneously. Their appearance in all eight transformed cell types studied suggests their ubiquity and involvement in transformation morphology. Actin patches developed in normal rat kidney (NRK) cells transformed by a temperature-sensitive mutant of Rous sarcoma virus (LA23-NRK) within 30 min after a shift from the nonpermissive (39°C) to the permissive temperature (32°C). Patch appearance paralleling viral src gene expression tends to implicate pp60^{src} kinase activity in destabilizing the cytoskeleton. However, appearance of the actin aggregates in cells not transformed by retrovirus calls for alternative mechanisms, perhaps involving an endogenous kinase, for this apparently common trait.

Phenotypic changes characteristic of transformed cells in vitro include alterations in cell morphology, growth rate, and metabolism (1). Rounded cell shape and loss of cell substrate anchorage are associated with transformation (2, 3) and tumorigenicity (4, 5) of fibroblasts in vitro. The cytoskeleton of transformed cells exhibits fewer distinct actin stress fibers, microfilaments, and microtubules and appears less ordered than the cytoskeleton in untransformed cells, an expected accompaniment of the morphological changes (3, 6–11).

In cells transformed by Rous sarcoma virus (RSV), the phenotypic changes including cell rounding, loss of anchorage, and cytoskeletal disorganization have been ascribed to changes in cytoskeletal proteins (12, 13), perhaps resulting from their phosphorylation by the src gene product, pp60^{src} (14, 15).

Motivated by the morphological and cytoskeletal changes induced by virus transformation and by the indications that the cytoskeleton may be a primary site for pp60^{src} activity, we have investigated the F-actin distribution in various transformed cells including those transformed by retroviruses. A small fluorescent probe, nitrobenzoxadiazole-phallacidin (NBD-Ph), that is highly specific for F-actin filaments and actin oligomers (16–20) permitted intense staining of F-actin and actin oligomers in cells after simple formaldehyde fixation, without extraction. F-actin binds up to one phallotoxin per actin molecule (21) and produces no nonspecific fluorescence discernible above the normal cellular autofluorescence.

We have stained the actin structures in cells transformed by RNA and DNA tumor viruses, and by chemical mutagens, and in cells transformed spontaneously. The F-actin stress fibers characteristic of untransformed cells are sparse or sometimes completely undetectable in the transformed cells. We have found that all types of transformed cells that we have stained with NBD-Ph display quite distinctive labeling patterns consisting primarily of actin patches near the ventral surface of the cell. The time-course of the changes of actin structures parallels the expected expression of the src gene in normal rat kidney (NRK) cells infected with a temperature-sensitive RSV mutant after shift to a transformation permissive temperature. Implications that actin patches may be characteristic of transformation and that phosphorylation of structural proteins by src gene products induces the cytoskeletal changes are discussed.

MATERIALS AND METHODS

Untransformed and Transformed Cell Cultures

Cell lines were maintained in Dulbecco's modified Eagle's medium containing 10% calf serum in an atmosphere of 10% CO_2 and 90% air at 37°C unless specified otherwise. For the differentially metastatic spontaneous B16 melanomas, F_0 and F_{10} mouse cells (22), fetal calf serum replaced calf serum. All cells were passaged using 0.05% trypsin in 0.01% EDTA in phosphate-buffered saline (PBS, pH 7.3), plated on glass coverslips at ~2×10^4 cells per 35-mm dish, and utilized in experiments only after 1–2 d of growth. All cells were obtained and cultured in the central tissue culture facility of the Cancer Research Center Program Project (CA 14454) and originated from the following sources: P. Vogt (University of California, Los Angeles, Calif.) supplied the transformation temperature-sensitive RSV-infected NRK cells (LA23-NRK; see reference 23), the B77(RSV)-infected NRK cells (B77-NRK[S]; originating from Dr. Louis Siminovitch, Ontario Cancer Institute, Toronto, Canada), and the Prague c strain (RSV)-infected NRK cells (Pr-NRK). A different cloned isolate of B77(RSV)-infected NRK cells (B77-NRK) and the NRK cells were obtained from R. Eisenman (Hutchinson Cancer Institute, Seattle, Wash.). Simian virus 40–infected mouse 3T3 cells (SV40-3T3) came from E. Rozengurt (Imperial Cancer Research Fund, Lincoln's Inn Fields, London, England). The F_0 and F_{10} differentially metastatic melanomas came from I. J. Fidler (Fredrick Cancer Research Center, Fredrick,

THE JOURNAL OF CELL BIOLOGY · VOLUME 90 SEPTEMBER 1981 797-802

Md.). Chicken embryo fibroblasts (CEF) from 6-d-old embryos were infected with a Schmidt-Rupin b strain of RSV (SR-b-CEF) from A. Goldberg (Rockefeller Institute, New York.). Kirsten murine sarcoma virus–transformed NRK cells (K-NRK) came from E. Scolnick (National Cancer Institute, Bethesda, Md.). W. B. Stallcup (Salk Institute, San Diego, Calif.) supplied the chemically induced mouse neuroblastoma clone (NB-CCL-1300-N18). All cell lines were found to be free of PPLO (mycoplasma) by culture assay.

NBD-Ph Staining

Washing buffers and labeling solutions were maintained and applied at the temperature of cell incubation. Cells on glass cover slips were washed twice in PBS, fixed in 3.7% formaldehyde (formalin) in PBS for 1 h at 20°C, incubated with 100 nM NBD-Ph (16) in PBS for 1 h at 20°C, washed three times in PBS, and mounted for viewing. A Nikon Optiphot epifluorescence microscope equipped with a × 100 phase-contrast objective provided fluorescence and phase-contrast images of cells. NBD fluorescence was excited by 450- to 480-nm illumination from an HBO 50-W mercury lamp (Osram; Macbeth Sales Corp., Newburgh, N. J.) with the exciting light blocked with a 515-nm barrier filter.

RESULTS

Initially we examined the microfilaments of NRK cells and their Rous sarcoma virus–transformed counterpart, the B77-NRK. Fig. 1 *a* shows a phase-contrast and *b* a fluorescence photomicrograph of the same untransformed NRK cells. In Fig. 1 *b*, the actin cables extending throughout the cell are clearly labeled by NBD-Ph, with little diffuse staining background. Cables of various sizes are stained, whereas no nuclear components fluoresce. NRK cells in the G_1, S, G_2, and M phases of the cell cycle were surveyed at random and exhibited stress fibers and microfilaments in all stages (not shown) except during late G_2 and mitosis. Rounded NRK cells in late G_2 or M contained very few microfilaments that stained with NBD-Ph. The majority of the fluorescence emanated from an intense diffuse pattern evenly distributed within the cell (Fig. 1 *e*). In many mitotic NRK cells, bright staining by NBD-Ph was also seen near the cytoplasmic face of the plasma membrane.

Fig. 1 *c* and *d* depicts phase-contrast and NBD-Ph-fluorescence photomicrographs of B77-NRK cells. These transformed NRK cells are rounded and have few extended cytoplasmic processes (Fig. 1 *c*). NBD-Ph staining of actin shows a small amount of diffuse background staining, but most of the fluorescence comes from a regular array of actin patches (Fig. 1 *d*).

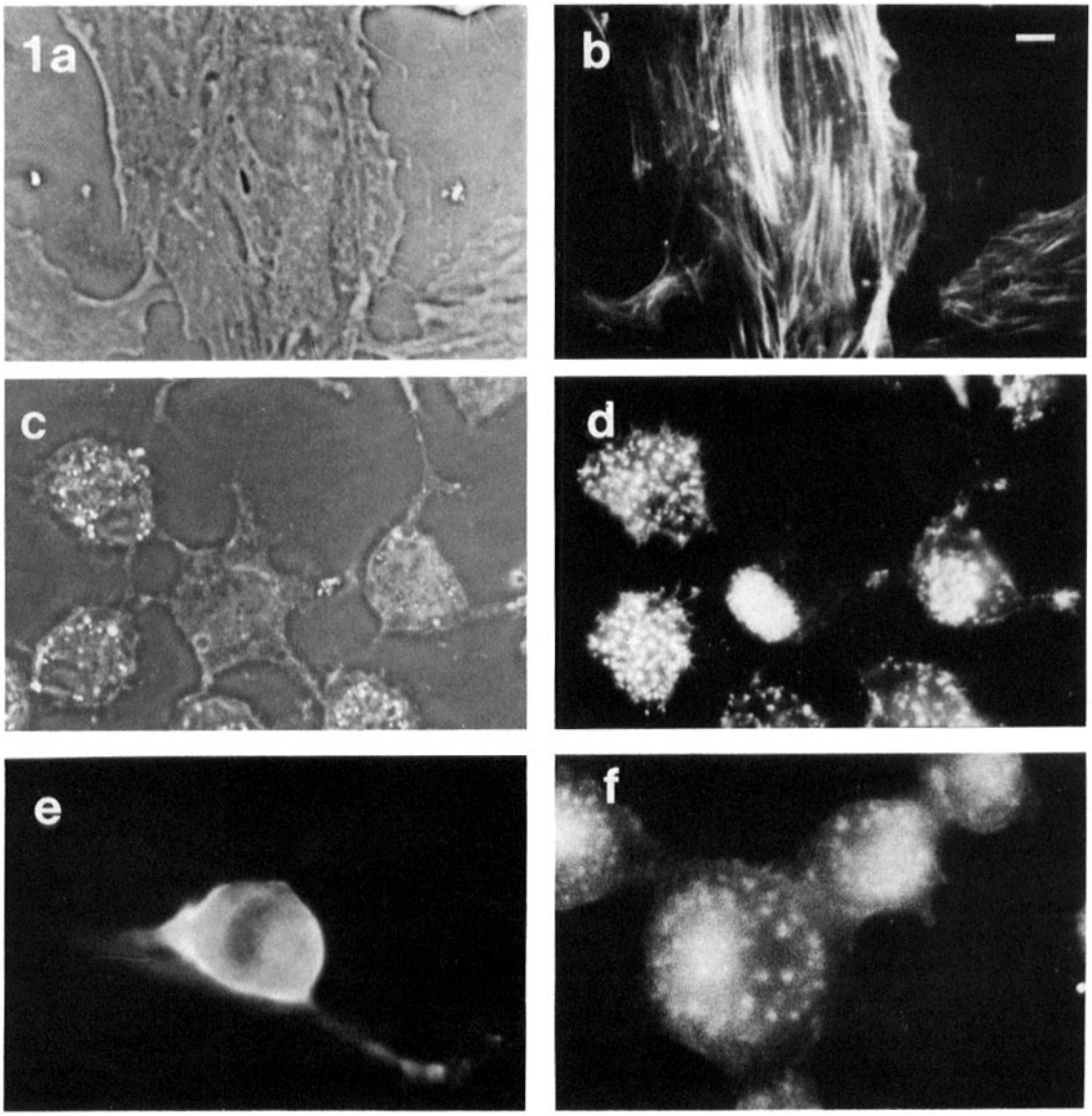

FIGURE 1 Staining of NRK and B77-NRK cells with NBD-Ph: (*a*) NRK cells, phase contrast; (*b*) NRK cells, fluorescence; (c) B77-NRK cells, phase contrast; (*d*) B77-NRK, fluorescence; (*e*) dividing NRK cells, fluorescence; (*f*) B77-NRK, DNase I-rhodamine, fluorescence. Cells were cultured, fixed, stained, and photographed as described in Materials and Methods. Bar, 10 μm.

These actin patch arrays appear in every B77-NRK cell and cover from 20 to 90% of the projected area of the cell. They are located close to the ventral surface of the cell and under the plane of the nucleus. We located the patch depth within the cell by focusing through the cell in phase and fluorescence. Patch location is therefore limited to a vertical resolution of ~1 μm. The number of patches per cell varies from ~30 to >100, with patch sizes ranging from 0.5 to 2 μm in diameter.

To determine whether the appearance of actin patches is a general consequence of viral transformation, we stained a

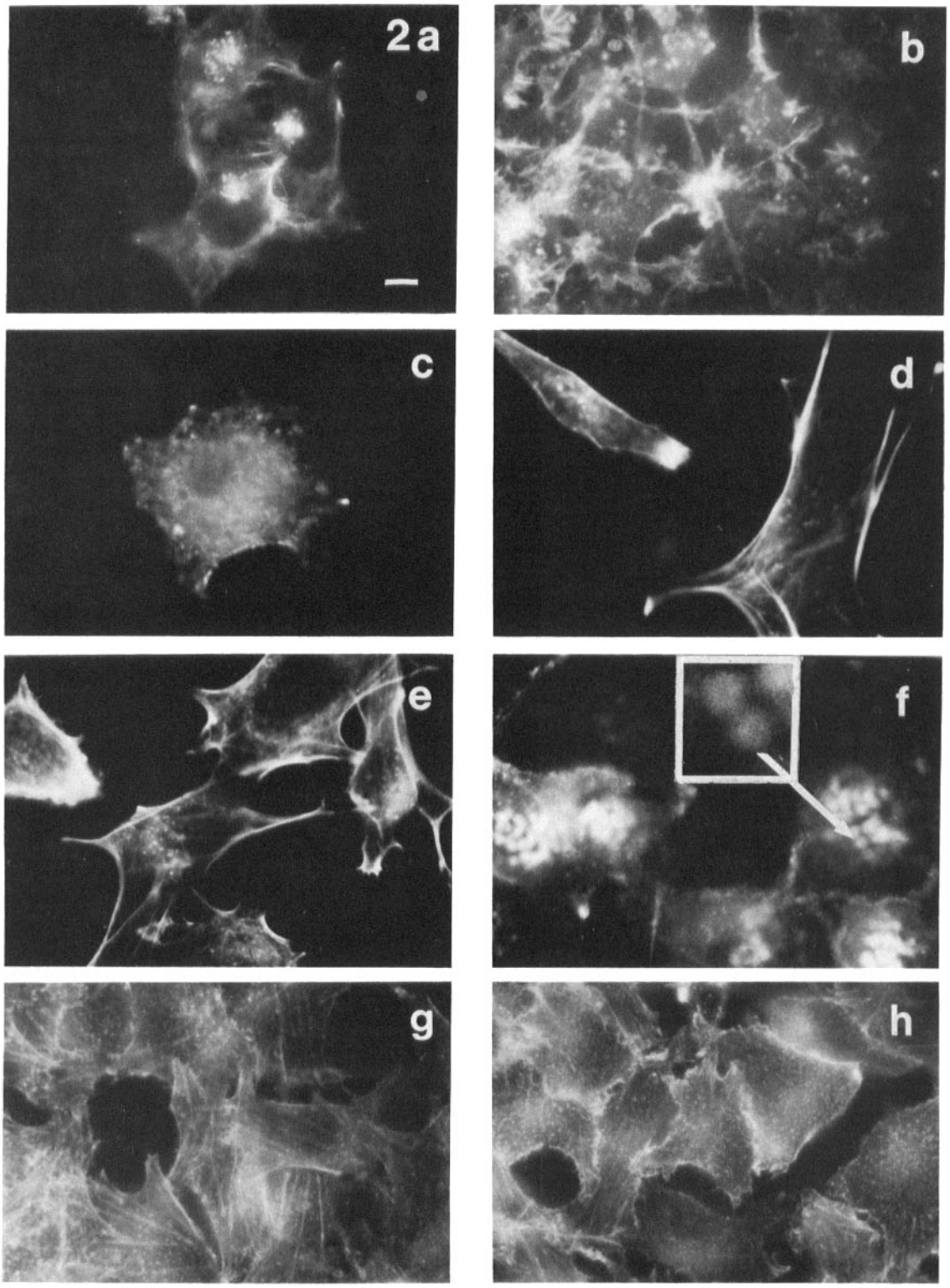

FIGURE 2 Staining of a variety of transformed cells with NBD-Ph: (*a*) Pr-NRK cells; (*b*) B77-NRK(S) cells; (*c*) K-NRK cells; (*d*) SR-b-CEF cells; (*e*) SV40-3T3 cells; (*f*) neuroblastoma cells; (*g*) F_0 (less metastatic) melanoma cells; (*h*) F_{10} (more metastatic) melanoma cells. Cells were cultured, fixed, stained, and photographed as described in Materials and Methods. Bar, 10 μm. *Inset* is enlarged six times, as compared with *f*.

variety of transformed cell types with NBD-Ph. Fig. 2 *a–h* illustrates the patch sizes and the degree to which various transformed cells exhibit actin patches and/or lack actin cables. Table I summarizes these observations. All of the transformed cell types contained actin patches.

NRK cells transformed with a Prague-c strain of RSV (Pr-NRK) (Fig. 2 *a*) contain patches that are located in the center of the cell. Patches range in size from 0.5 to 1 μm and number ~50 patches per cell. These cells contain very few actin cables. A different clonal isolate of NRK cells infected with RSV (B77-NRK[S]) exhibits a more diffuse array of actin patches that vary from ≤0.2 to 2.0 μm in diameter. These cells contain roughly the same number of patches per cell and more cables than Pr-NRK cells (Fig. 2 *b*). In NRK cells transformed by a Kirsten murine sarcoma virus (K-NRK), patches are evident only near the periphery of the cell; these patches are 0.5–2 μm in diameter. Those patches near the center of the K-NRK cells are partially obscured by diffuse staining that may arise from patch overlap or from an actin distribution that is actually diffuse on the scale of the microscope resolution. No cables are observed (Fig. 2 *c*). In all of these transformed NRK cells, the characteristic actin patches were reproducibly present in at least 90% of all cells inspected.

Patches and some cables are also seen in primary CEF cells that are transformed with a Schmidt-Rupin b strain of RSV (SR-b-CEF) (Fig. 2 *d*). The size range (≤0.2–1 μm) and number of patches per cell are similar to those of the transformed NRK cells. In these cells, however, the patch appearance and distribution is less distinctive and was detectable by fluorescence microscopy in only 75% of the cells examined. Murine 3T3 fibroblasts transformed by a DNA virus, SV40, contain actin patches and cables that appear in sizes and intracellular distributions (Fig. 2 *e*), similar to those of SR-b-CEF cells. The transformation-characteristic patching was detected in only ~75% of the transformed cell population. Untransformed chick embryo fibroblasts and 3T3 fibroblasts do not exhibit patches when stained with NBD-Ph (not shown).

A chemically induced neuroblastoma cell line (Fig. 2 *f*) displays a distinct array of patches, which appear highly ordered and uniformly large sized (2–4 μm in diameter), and contains few actin cables. Many of these patches appear hollow in the center and could be described as rosettes. (see *inset* in Fig. 2 *f*). We also stained two sustained mouse melanoma cell lines which have been selected by Fidler (22) for different metastatic potential. The F_0 cell has the lowest metastatic potential while F_{10} cell has the highest. Fig. 2 *g* and *h* show NBD-Ph staining in the F_0 and F_{10} cells, respectively. Although the F_0 cells do contain actin patches they also contain numerous actin cables; the F_{10} cells, however, display many more actin patches and fewer actin cables. These transformation-characteristic actin patches were reproducibly observed in at least 90% of the cell populations of both the melanomas and the neuroblastomas.

To observe cytoskeletal collapse directly as a function of src gene product activity, we used NRK cells infected with a mutant RSV that is temperature sensitive for the transformed phenotype (LA23-NRK) (23). Photomicrographs illustrating the time-course of actin patch appearance after a temperature shift (39° → 32°C) are shown in Fig. 3 *a–e*. Fig. 3 *a* is a fluorescence micrograph of LA23-NRK at 39°C that exhibits many typical actin cables and microfilaments similar to those seen in untransformed NRK cells. Actin patches appearing on the ventral cell surface increase in number the longer the cells remain at the permissive temperature. They occur in ~30% of the cells after 15 min (Fig. 3 *b*) and in ~90% after 30 min (Fig. 3 *c*) and continue to increase in number and size (Fig. 3 *d*). As actin patches appear throughout this time-course, stress fibers become sparser in the center of the cell. The F-actin aggregations at the cell periphery, especially at cell-cell contacts, are sometimes retained or enhanced (Fig. 3 *b*). Later, as rounding occurs, actin patches concentrate near the cell center and only peripheral F-actin fragments remain at the boundary (Fig. 3 *d*, arrow). Finally, after 2.5 h, many of the cells (>90%) have a large number (>100) of actin patches, and some of them (~10–15) show a full rounded morphology like the B77-NRK cells (Fig. 3 *e*). As controls, both NRK and RSV-transformed NRK cells were taken through the same time-course after the temperature shift. In the RSV-transformed cells the number of patches was not affected by the shift. Actin patches were not visible in any of the NRK cells shifted to 32°C (not shown).

TABLE I

Actin Patch and Cable Characteristics of Transformed Cells

Cell line	Patch location in the cell	Patch size* range (average)	Patch number‡/ cell (10-cell average)	Cable structure presence§
		μm		
B77-NRK	Sometimes center; mostly throughout cell	0.5–2 (~2)	40	0–5
Pr-NRK	Center	0.5–1 (~1)	30	5–10
B77-NRK(S)	Central (diffuse)	0.2–1 (~1)	30	10–20
K-NRK	Edges (diffuse)	0.2–2 (~1)	>100‖	0–5
Neuroblastoma	Center	2–4 (~4)¶	20	5–10
SR-b-CEF	Central	0.2–1 (~1)	40	5–10
SV40-3T3	Central	0.5–2 (~1)	20	5–10
F_0	Throughout	0.2–1 (~1)	60	>20
F_{10}	Throughout	0.2–1 (~1)	110	10–20

Transformed cells were cultured, stained, and photographed as described in Materials and Methods. The distributions given are representative of subconfluent as well as confluent attached transformed cells.

* Patch size range was calculated by measuring the diameter of the smallest and largest discernible patch in 10 cells. The average size patch represents 70% or more of the patch in 10 cells. Optical resolution of ~0.2 μm implies ≤0.2-μm patch sizes.

‡ The number of patches per cell is an average from counting 10 cells and can vary up to 40% for each number given.

§ The number of cables per cell is the range found on counting 10 cells.

‖ This number is a rough estimate because in many of the cells counted the individual patches were not clearly discernible.

¶ These patches appeared large with hollow centers and resembled rosettes (see *inset* in Fig. 2 *f*).

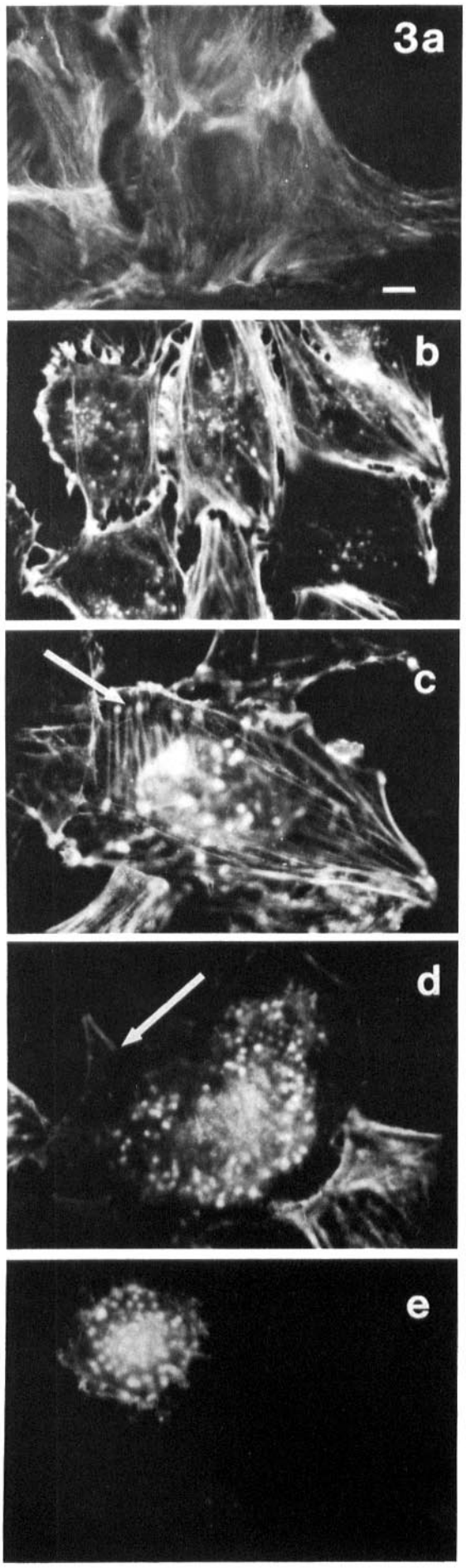

To ensure that NBD-Ph did not induce patch formation by promoting actin polymerization, we stained fixed-extracted B77-NRK cells with NBD-Ph or DNase I conjugated to rhodamine (DNase I–Rh) (20). DNase I–Rh penetrated fixed-extracted cells and stained actin patches similar to those seen with NBD-Ph (Fig. 1*f*). However, a diffuse background presumably caused by G-actin staining often obscured patches in the center of the B77-NRK cells. These results rule out the possibility that the actin patches we observed with NBD-Ph in fixed transformed cells are an artifact, because DNase I–Rh does not induce actin polymerization (24) and does reveal actin patches in fixed-extracted transformed cells.

DISCUSSION

The F-actin specific fluorescent toxin NBD-Ph stained actin stress fibers and microfilaments in untransformed cells except in G_2 and mitosis, as expected from previous studies with other actin markers (3, 7, 8). (For details of NBD-Ph staining in G_2 and mitosis, see Barak et al. [20].) In the various transformed cells studied, NBD-Ph stained few actin cables and filaments but did stain distinctive, transformation-characteristic F-actin structures consisting of numerous patchy aggregates located near the ventral surfaces.

The F-actin aggregate sizes and distributions depend on cell type and transforming virus (Fig. 2*a–h* and Table I). In all of the transformed cell lines examined, except SR-b-CEF and SV40-3T3 cells, actin patches were found in at least 90% of the cell population. In some cases the actin aggregates are grouped near the cell center, particularly in the Pr-NRK cells (Fig. 2*a*). In others, particularly B77-NRK (Fig. 1*d*), intracellular distribution of actin patches varies substantially from cell to cell.

In the differentially metastatic melanoma cells, the actin patches are particularly uniform in size and distribution and are apparently coplanar. F-actin also appears to be concentrated along F_{10} cell peripheries, especially at cell-cell contacts. The higher metastatic potential F_{10} appears to be a more completely transformed phenotype with fewer remaining visible actin cables and more patches (Fig. 2*h* and *g*).

The characteristics of the actin patches in SV40-3T3 and SR-B-CEF cells were not typical of the group of transformed cells studied. They were generally less distinctive and less apparent. In SV40-3T3 cells, there were fewer patches per cell; they were sometimes relatively small and were detected in only 75% of the cell population. Verderame et al. (11) have recently reported observations of the attenuation of fibrous actin structures in SV40-3T3 cells stained with F-actin-specific fluorescein-labeled phalloidin. However, they do not report actin patches in these transformed cells, perhaps because the relatively weak expression of the effect in this case was not visible after the permeabilization procedure used for this stain. In SR-B-CEF cells, similar patching was observed and was detectable in only 75% of the cell population. In this case some of the cells may have remained untransformed, and therefore patchless, because the cells were studied within two generations after infection to avoid tissue culture artifacts.

Using temperature-sensitive virus-infected NRK cells

FIGURE 3 Staining of LA23-NRK cells with NBD-Ph after a shift from the nonpermissive (39°C) to the permissive temperature (32°C): (*a*) LA23-NRK, 39°C; (*b*) LA23-NRK, 32°C, 15 min after shift; (*c*) LA23-NRK, 32°C, 30 min after shift; (*d*) LA23-NRK, 32°C, 1 h after shift; (*e*) LA23-NRK, 32°C, 2 h after shift. Cells were cultured, fixed, stained, and photographed as described in Materials and Methods. Bar, 10 μm. × 630.

(LA23-NRK), we monitored the time-course of actin patch aggregation in these cells after a temperature shift from 39° (nonpermissive) to 32°C (permissive). Changes in surface topography and cell morphology, and loss of microfilament organization induced by a temperature shift had been reported using similar viral mutants (7, 8). These changes were evident 1–2 h after a shift to the permissive temperature (8) and resembled changes in the microfilament system in untransformed cells entering late G_2 or M phases of the cell cycle. We observed a similar loss of actin cables and microfilaments after a temperature shift in LA23-NRK cells. In addition, we have observed that numerous prominent actin patches appeared soon after a temperature shift to the permissive temperature (Fig. 3 *b–e*). Proliferation of patches was evident (Fig. 3 *b* and *c*) 15–30 min after temperature shifts, indicating that actin patch formation is an early result of src gene expression. Fig. 3 *c*, 30 min after the shift, shows that the patches may occur at the ends of some of the filaments rather like adhesion plaques in cells (see arrow in Fig. 3 *d*.)

Rohrschneider (15) has recently reported that $pp60^{src}$ appears in RSV-transformed cells as plaques at areas of close cell contact with the substratum that are detected by interference contrast microscopy. These plaques, stained for $pp60^{src}$ by indirect immunofluorescence, resemble the actin patches we have stained near the ventral surfaces of similar transformed cells (Figs. 1 *d* and 2 *b*). However, David-Pfeuty and Singer (14) have found that vinculin and α-actinin, present in the adhesion plaques of untransformed fibroblasts, appear near the ventral surface of RSV-transformed fibroblasts as large patches and as clusters of patches that are not necessarily coincident with adhesion plaques. These patches also resemble the actin patches that we have observed, in both distribution and size. Whether our actin patches, the $pp60^{src}$ plaques reported by Rohrschneider (15), and the vinculin/α-actinin patches reported by David-Pfeuty and Singer (14) are related awaits results of colabeling experiments. The possibility is suggested by the finding by Sefton and co-workers (unpublished results mentioned in reference 14) that vinculin is a $pp60^{src}$ substrate. Tyrosine phosphorylation on vinculin by $pp60^{src}$ may alter vinculin-microfilament interactions in adhesion plaques and thereby catalyze microfilament collapse. This mechanism could account for actin aggregation into patches, particularly in permissively shifted LA23-NRK cells, where they were found at microfilament termini. This hypothesis does not, however, account for similar actin patches observed in cells such as SV40-3T3, neuroblastoma, and F_0 and F_{10} melanomas that were not transformed by retrovirus and thus are not known to contain a viral encoded src gene protein kinase. Whether this apparently common trait of actin patching upon transformation is attributable to a common mechanism such as a hierarchy of kinases (25, 26) may be discernible by identification of other patch-associated proteins. In any case we can regard the patches of cytoskeletal proteins in transformed cells as detritus from collapse of the fibrous cytoskeleton.

Our results indicate that characteristic actin patches occur in a variety of transformed cells irrespective of the cause of transformation. Although presently supported by only a narrow range of transformed cells, patch formation may be a common trait of transformed cells and may provide clues to the mechanisms underlying the phenotypic changes in transformed cells.

We thank Gene Nothnagel for the synthesis of the DNase I-Rh and for helpful discussions. We gratefully acknowledge the contributions of Diana Wescott, Mary Lipsky, and Beth Lane for the growth, preparation, and mycoplasma screening of the transformed cells described herein.

These studies were supported by National Institutes of Health (NIH) grant GM 21661, NIH Cancer Research Center Program Project grant CA 14454, and National Science Foundation grant PCM 8007-637.

Received for publication 13 April 1981, and in revised form 20 May 1981.

REFERENCES

1. Hanafusa, H. 1977. Cell transformation by RNA tumor viruses. *In* Comprehensive Virology. H. Fraenkel-Conrat and R. P. Wagner, editors. Plenum Publishing Corp., New York. 10:401–483.
2. Hsie, A. W., and T. T. Puck. 1971. Morphological transformation of Chinese hamster cells by dibutryl adenosine cyclic 3′:5′-monophosphate and testosterone. *Proc. Natl. Acad. Sci. U. S. A.* 68:358–361.
3. Pollack, R., M. Osborn, and K. Weber. 1975. Patterns of organization of actin and myosin in normal and transformed cultured cells. *Proc. Natl. Acad. Sci. U. S. A.* 72:994–998.
4. Shin, S., V. H. Freedman, R. Risser, and R. Pollack. 1975. Tumorigenicity of virus-transformed cells in nude mice is correlated specifically with anchorage independent growth *in vitro*. *Proc. Natl. Acad. Sci. U. S. A.* 72:4435–4439.
5. Freedman, V. H., and S. Shin. 1974. Cellular tumorigenicity in nude mice: correlation with cell growth in semi-solid medium. *Cell.* 3:355–359.
6. Brinkley, B. R., G. M. Fuller, and D. P. Highfield. 1975. Cytoplasmic microtubules in normal and transformed cells in culture: analysis by tubulin antibody immunofluorescence. *Proc. Natl. Acad. Sci. U. S. A.* 72:4981–4985.
7. Wang, W., and A. R. Goldberg. 1976. Changes in microfilament organization and surface topography upon transformation of chick embryo fibroblasts with Rous sarcoma virus. *Proc. Natl. Acad. Sci. U. S. A.* 73:4065–4069.
8. Edelman, G., and I. Yahara. 1976. Temperature-sensitive changes in surface modulating assemblies of fibroblasts transformed by mutants of Rous sarcoma virus. *Proc. Natl. Acad. Sci. U. S. A.* 73:2047–2051.
9. Pollack, R., and D. B. Rifkin. 1976. Modification of mammalian cell shape: redistribution of intracellular actin by SV40 virus, proteases, cytochalasin B and dimethylsulfoxide. *In* Cell Motility. R. Goldman, T. Pollard, and J. Rosenbaum, editors. Cold Spring Harbor Laboratory, Cold Spring Harbor, N.Y. A:389–401.
10. Meek, W. D., and T. T. Puck. 1979. Role of the microfibrillar system in knob actin of transformed cell. *J. Supramol. Struct.* 12:335–354.
11. Verderame, M., D. Alcorta, M. Egnor, K. Smith, and R. Pollack. 1980. Cytoskeletal F-actin patterns quantitated with fluorescein isothiocyanate-phalloidin in normal and transformed cells. *Proc. Natl. Acad. Sci. U. S. A.* 77:6624–6628.
12. Erickson, R. L., A. F. Purchio, E. Erickson, M. S. Collett, and J. S. Brugge. 1980. Molecular events in cells transformed by Rous sarcoma virus. *J. Cell Biol.* 87:319–325.
13. Hunter, T., and B. Sefton. Protein kinases and viral transformation. *In* Molecular Aspects of Cellular Recognition. II. The Molecular Actions of Toxins, Viruses, and Interferon. P. Cohen and S. Van Heyniger, editors. Elsiever/North Holland, Amsterdam. In press.
14. David-Pfeuty, T., and S. J. Singer. 1980. Altered distribution of the cytoskeletal proteins vinculin and α-actinin in cultures fibroblasts transformed by Rous sarcoma virus. *Proc. Natl. Acad. Sci. U. S. A.* 77:6687–6691.
15. Rohrschneider, L. R. 1980. Adhesion plaques of Rous sarcoma virus-transformed cells contain the src gene product. *Proc. Natl. Acad. Sci. U. S. A.* 77:3514–3518.
16. Barak, L. S., R. R. Yocum, E. A. Nothnagel, and W. W. Webb. 1980. Fluorescence staining of the actin cytoskeleton in living cells with 7-nitrobenz-2-oxa-'3-diazole-phallacidin. *Proc. Natl. Acad. Sci. U. S. A.* 77:980–984.
17. Barak, L. S., and R. R. Yocum. 1981. Nitrobenzoxazole-phallacidin: Synthesis of a fluorescent actin probe. *Anal. Biochem.* 110:31–38.
18. Nothnagel, E. A., L. S. Barak, J. W. Sanger, and W. W. Webb. 1981. Fluorescence studies on modes of cytochalasin B and phallotoxin action on cytoplasmic streaming in *Chara*. *J. Cell Biol.* 88:364–372.
19. Barak, L. S., R. R. Yocum, and W. W. Webb. 1981. In vivo staining of cytoskeletal actin by autointernalization of nontoxic concentrations of nitrobenzoxadiazole-phallacidin. *J. Cell Biol.* 89:368–372.
20. Barak, L. S., E. A. Nothnagel, E. F. De Marco, and W. W. Webb. 1981. Differential staining of actin in metaphase spindles with NBD-phallacidin and fluorescent deoxyribonuclease: is actin involved in chromosomal movement? *Proc. Natl. Acad. Sci. U. S. A.* 78(5):3034–3038.
21. Wieland, Th., and H. Faulstich. 1978. Amatoxins, phallatoxins, phallolysin and antamanide: the biologically active components of poisonous amanita mushrooms. *CRC Crit. Rev. Biochem.* 5:185–260.
22. Fidler, I. J. 1973. Selection of successive tumor lines for metastasis. *Nature (New Biol.).* 242:148–149.
23. Ash, J. F., P. K. Vogt, and S. J. Singer. 1976. Reversion from transformed to normal phenotype by inhibition of protein synthesis in rat kidney cells infected with a temperature-sensitive mutant of Rous sarcoma virus. *Proc. Natl. Acad. Sci. U. S. A.* 73:3603–3607.
24. Hitchcock, S. E., L. Carlsson, and U. Lindberg. 1976. DNase I-induced depolymerization of actin filaments. *In* Cell Motility. R. Goldman, T. Pollard, and J. Rosenbaum, editors. Cold Spring Harbor Laboratory, Cold Spring Harbor, N.Y. B:545–559.
25. Spector, M., S. O'Neal, and E. Racker. 1980. Phosphorylation of the β subunit of Na^+K^+ATPase in Ehrlich ascites tumor by a membrane-bound protein kinase. *J. Biol. Chem.* 255:8370–8373.
26. Spector, M., S. O'Neal, and E. Racker. 1981. Regulation of Phosphorylation of the β subunit of the Ehrlich ascites tumor Na^+K^+ATPase by a protein kinase cascade. *J. Biol. Chem.* 256:4219–4227.